Supplementary of

Assessment of a multi-tiling energy budget approach in a land surface model, ORCHIDEE-MICT (r8205)

Yi Xi[1], Chunjing Qiu[2,3], Yuan Zhang[4,1], Dan Zhu[5], Shushi Peng[5], Gustaf Hugelius[6], Jinfeng Chang[7], Elodie Salmon[1], Philippe Ciais[1]

[1]Laboratoire des Sciences du Climat et de l'Environnement, LSCE/IPSL, CEA – CNRS – UVSQ, Université Paris-Saclay, 91191 Gif-sur-Yvette, France
[2]Research Center for Global Change and Complex Ecosystems, School of Ecological and Environmental Sciences, East China Normal University, Shanghai, China.
[3]Institute of Eco-Chongming, East China Normal University, Shanghai, China
[4]Key Laboratory of Alpine Ecology, Institute of Tibetan Plateau Research, Chinese Academy of Sciences, Beijing 100101, China;
[5]Sino-French Institute for Earth System Science, College of Urban and Environmental Sciences, Peking University, Beijing 100871, China
[6]Department of Physical Geography, Stockholm University, Stockholm, Sweden
[7]College of Environmental and Resource Sciences, Zhejiang University, Hangzhou, China

Correspondence to: Yi Xi (yi.xi@lsce.ipsl.fr)

Table S1. The vertical discretization of soil layers in ORCHIDEE-MICT. There are 11 soil layers for hydrology and 32 soil layers for thermal in the model, and the depth of 11 hydrologic layers is identical to that of the first 11 thermal layers. The thermal layers in red are selected to show the difference in thermal and hydrologic variables between MICT-teb and MICT in Figs. 8-9, S9-S13.

Hydrology		Thermal	
Soil layer	**Depth (m)**	**Soil layer**	**Depth (m)**
1	0.0010	1	0.0010
2	0.0039	2	0.0039
3	0.0098	3	0.0098
4	0.0215	4	0.0215
5	0.0450	5	0.0450
6	0.0919	6	0.0919
7	0.1857	7	0.1857
8	0.3734	8	0.3734
9	0.7488	9	0.7488
10	1.4995	10	1.4995
11	2.0000	11	2.0000
		12	3.0010
		13	4.0270
		14	5.1043
		15	6.2354
		16	7.4232
		17	8.6703
		18	9.9798
		19	11.3547
		20	12.7984
		21	14.3143
		22	15.9059
		23	17.5772
		24	19.3320
		25	21.1745
		26	23.1092
		27	25.1406
		28	27.2736
		29	29.5132
		30	31.8649
		31	34.3341
		32	38.0000

Table S2. Minimum snow albedo value after aging (α_{snow_min}) and decay rate (k) of 16 plant function types (PFT) used in ORCHIDEE-MICT. Both visible and near infrared albedo are shown.

PFT	α_{snow_min}			k		
	Visible	Near infrared	Average	Visible	Near infrared	Average
1. Bare soil	0.35	0.35	0.35	0.45	0.45	0.45
2. Tropical broad-leaved evergreen	0	0	0	0	0	0
3. Tropical broad-leaved raingreen	0	0	0	0	0	0
4. Temperate needleleaf evergreen	0.14	0.14	0.14	0.1	0.06	0.08
5. Temperate broad-leaved evergreen	0.14	0.14	0.14	0.06	0.06	0.06
6. Temperate broad-leaved summergreen	0.14	0.14	0.14	0.11	0.11	0.11
7. Boreal needleleaf evergreen	0.14	0.14	0.14	0.10	0.06	0.08
8. Boreal broad-leaved summergreen	0.14	0.14	0.14	0.11	0.11	0.11
9. Boreal needleleaf summergreen	0.14	0.14	0.14	0.18	0.11	0.145
10. Temperate C3 grass	0.18	0.18	0.18	0.60	0.52	0.56
11. C4 grass	0.18	0.18	0.18	0.60	0.52	0.56
12. Wheat	0.18	0.18	0.18	0.60	0.52	0.56
13. Maize	0.18	0.18	0.18	0.60	0.5	0.55
14. Tropical C3 grass	0.18	0.18	0.18	0.60	0.52	0.56
15. Boreal C3 grass	0.18	0.18	0.18	0.60	0.52	0.56
16. Peat C3 grass	0.18	0.18	0.18	0.60	0.52	0.56

Table S3. Visible and near infrared albedo of 15 plant function types (PFT) used in ORCHIDEE-MICT. The "Albedo" in the last column represents the average of visible and near infrared albedo.

PFT	Visible albedo	Near infrared albedo	Albedo
2. Tropical broad-leaved evergreen	0.0397	0.227	0.13335
3. Tropical broad-leaved raingreen	0.0474	0.214	0.13070
4. Temperate needleleaf evergreen	0.0386	0.193	0.11580
5. Temperate broad-leaved evergreen	0.0484	0.208	0.12820
6. Temperate broad-leaved summergreen	0.0411	0.244	0.14255
7. Boreal needleleaf evergreen	0.0410	0.177	0.10900
8. Boreal broad-leaved summergreen	0.0541	0.218	0.13605
9. Boreal needleleaf summergreen	0.0435	0.213	0.12825
10. Temperate C3 grass	0.0524	0.252	0.15220
11. C4 grass	0.0508	0.265	0.15790
12. Wheat	0.0509	0.272	0.16145
13. Maize	0.0606	0.244	0.15230
14. Tropical C3 grass	0.0524	0.252	0.15220
15. Boreal C3 grass	0.0524	0.252	0.15220
16. Peat C3 grass	0.0524	0.252	0.15220

Table S4. Roughness height of 16 plant function types (PFT) used in ORCHIDEE-MICT.

PFT	Roughness height (m)
1. Bare soil	0
2. Tropical broad-leaved evergreen	10.2
3. Tropical broad-leaved raingreen	10.2
4. Temperate needleleaf evergreen	6.8
5. Temperate broad-leaved evergreen	6.8
6. Temperate broad-leaved summergreen	6.8
7. Boreal needleleaf evergreen	5.1
8. Boreal broad-leaved summergreen	5.1
9. Boreal needleleaf summergreen	5.1
10. Temperate C3 grass	0.17
11. C4 grass	0.204
12. Wheat	0.34
13. Maize	0.34
14. Tropical C3 grass	0.17
15. Boreal C3 grass	0.17
16. Peat C3 grass	0.17

Table S5. Correlation coefficients (R) between differences in T_{snow} (ΔT_{snow}) and T_{surf} (ΔT_{surf}), or c_{snow} (Δc_{snow}), or λ_{snow} ($\Delta\lambda_{snow}$) for each snow layer and the snow depth weighted results. The numbers in red indicate the maximum coefficient among the three factors. The numbers in bold indicate the correlation coefficients are statistically significant ($p < 0.05$).

R	Layer 1			Layer 2			Layer 3			Snow depth weighted		
	ΔT_{surf}	Δc_{snow}	$\Delta\lambda_{snow}$	ΔT_{surf}	Δc_{snow}	$\Delta\lambda_{snow}$	ΔT_{surf}	Δc_{snow}	$\Delta\lambda_{snow}$	ΔT_{surf}	Δc_{snow}	$\Delta\lambda_{snow}$
Grid-cell mean	**0.17**	**-0.09**	**-0.08**	**0.12**	-0.03	-0.03	**0.09**	0.03	**0.05**	**0.09**	0.02	**0.04**
Bare soil	**0.23**	**0.10**	**0.21**	**0.09**	**0.12**	**0.22**	0.04	**0.14**	**0.22**	**0.07**	**0.13**	**0.24**
Tree	**0.60**	**-0.14**	-0.06	0.04	**0.37**	**0.40**	**-0.29**	**0.57**	**0.55**	**-0.13**	**0.46**	**0.49**
Grass	**0.69**	**0.16**	**0.23**	**0.50**	**0.32**	**0.40**	**0.19**	**0.41**	**0.44**	**0.38**	**0.36**	**0.42**
Peat grass	**0.16**	-0.02	0.03	**0.33**	**-0.26**	**-0.25**	**0.33**	**-0.20**	**-0.20**	**0.26**	**-0.14**	**-0.13**

Table S6. Correlation coefficients (R) between differences in T_{soil} (ΔT_{soil}) and T_{surf} (ΔT_{surf}, for 0-30N) / the temperature at the third snow layer ($\Delta T_{snow,3}$, for 30N-90N), or c (Δc), or λ ($\Delta\lambda$) for four soil layers. The numbers in red indicate the maximum coefficient among the three factors. The numbers in bold indicate the correlation coefficients are statistically significant ($p < 0.05$).

R	Latitudes	Layer 1 (0.0005 m)			Layer 9 (0.56 m)			Layer 11 (1.72 m)			Layer 32 (36.17 m)		
		ΔT_{surf} or $\Delta T_{snow,3}$	Δc	$\Delta\lambda$	ΔT_{surf} or $\Delta T_{snow,3}$	Δc	$\Delta\lambda$	ΔT_{surf} or $\Delta T_{snow,3}$	Δc	$\Delta\lambda$	ΔT_{surf} or $\Delta T_{snow,3}$	Δc	$\Delta\lambda$
Grid-cell mean	30N-90N	**0.31**	**-0.29**	**-0.07**	**0.32**	**0.34**	**-0.29**	**0.32**	**0.10**	**-0.24**	**0.30**	-0.02	**-0.36**
	0-30N	**1.00**	0.00	**0.44**	**1.00**	-0.02	**0.22**	**1.00**	**0.11**	**0.19**	**0.98**	**0.17**	**-0.05**
Bare soil	30N-90N	**0.34**	**-0.14**	**-0.09**	**0.38**	**-0.06**	**0.06**	**0.33**	**-0.14**	**0.09**	**0.39**	-0.03	**-0.14**
	0-30N	**1.00**	**-0.17**	**0.77**	**1.00**	-0.03	**0.75**	**1.00**	**0.11**	**0.31**	**0.99**	**0.25**	**0.19**
Tree	30N-90N	**0.77**	**-0.12**	**-0.09**	**0.76**	**-0.04**	**-0.09**	**0.75**	**-0.09**	**-0.24**	**0.68**	**-0.45**	**-0.56**
	0-30N	**1.00**	**-0.23**	**0.49**	**1.00**	-0.07	**0.50**	**1.00**	**0.08**	**0.19**	**0.90**	**-0.13**	**-0.19**
Grass	30N-90N	**0.74**	**-0.19**	**0.05**	**0.69**	**-0.31**	**0.11**	**0.62**	**-0.37**	**0.18**	**0.59**	**-0.36**	**-0.47**
	0-30N	**1.00**	**-0.28**	**0.38**	**1.00**	0.00	**0.75**	**1.00**	**0.22**	**0.49**	**0.96**	**0.32**	**0.27**
Peat grass	30N-90N	**0.66**	**-0.17**	**-0.60**	**0.54**	**-0.15**	**-0.44**	**0.41**	0.00	**-0.17**	**0.45**	**0.28**	**-0.26**
	0-30N	**1.00**	**-0.28**	-0.09	**0.99**	**-0.42**	**-0.21**	**0.97**	**-0.40**	0.12	**0.92**	-0.03	-0.06

Figure S1. Soil albedo from MODIS.

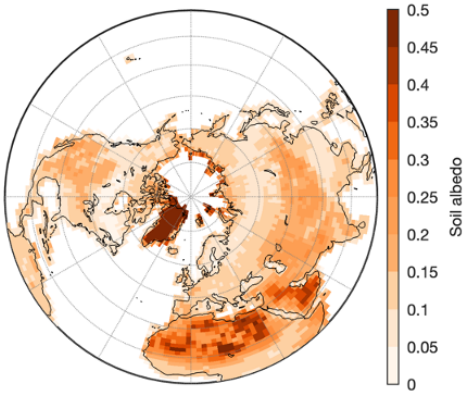

Figure S2. Comparison of vertical SOC profile (0-3 m) across different land cover types between site-level data from Palmtag et al., (2022) and simulation from ORCHIDEE-MICT. (a), Spatial distribution of 16 sites used in Palmtag et al., (2022). (b), The vertical profile of mean SOC density across all sites for 10 land cover types (DBF: deciduous broadleaf forest; ENF: evergreen needleleaf forest; DNF: deciduous needleleaf forest; Shrub: shrub tundra; Graminoid: graminoid / forb tundra; PerWet: permafrost wetlands; NPWet: non-permafrost wetland; Barren: barren; YeTundra: yedoma tundra; Yeforest: yedoma forest) from Palmtag et al., (2022). (c), The vertical profile of mean SOC density across all sites for 16 PFT from ORCHIDEE-MICT.

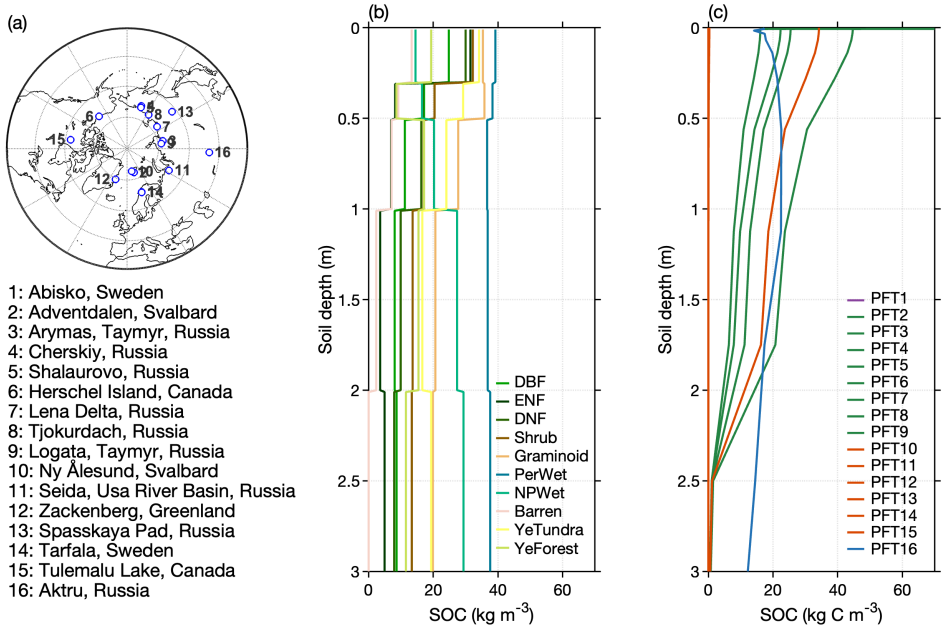

Figure S3. Comparison of spatial pattern of SOC for 0-3 m from observation-based data as used in Zhu et al. (2019) and simulation from ORCHIDEE-MICT.

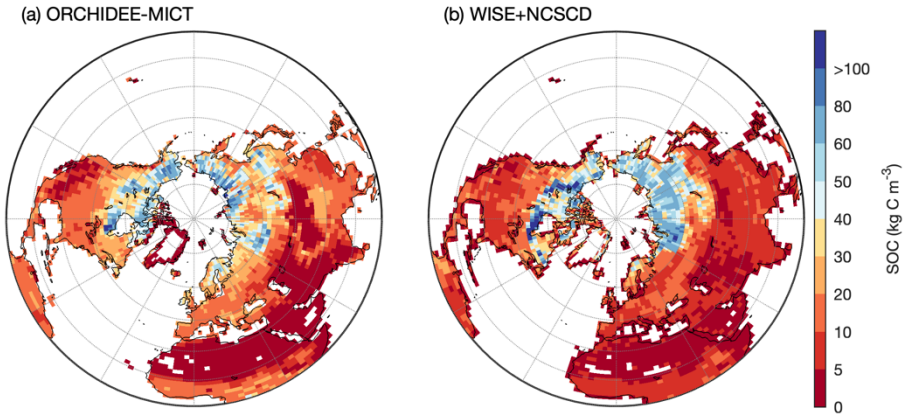

Figure S4. Same as Fig. 3, but for difference in snow cover fraction (f_{snow}) between MICT-teb and MICT for two grid-cells located at temperate (51°N, 101°W) and boreal (71°N, 147°E) regions, respectively.

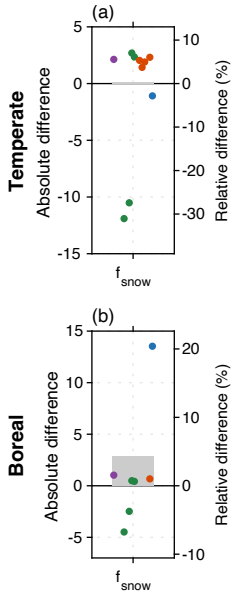

Figure S5. Spatial patterns of differences in snow cover fraction (f_{snow}) between MICT-teb and MICT over the Northern Hemisphere.

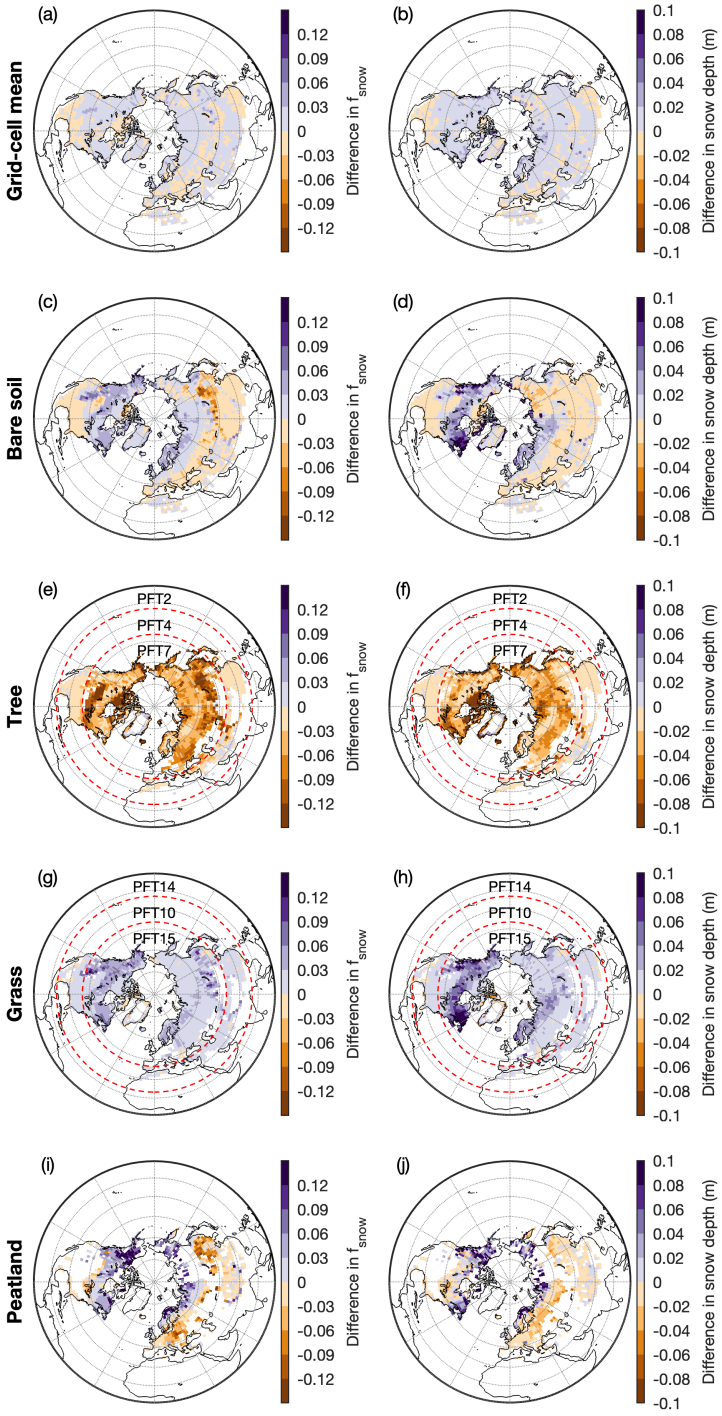

Figure S6. Same as Fig. 6, but for scatter plot of differences in surface properties between MICT-teb and MICT versus vegetation cover fraction for bare soil (PFT1), tree (PFT7), grass (PFT15), and peatland grass (PFT16). The surface properties include albedo (Albedo), surface temperature (T_{surf}), surface drag coefficients (C_d), and roughness height (H_{rough}).

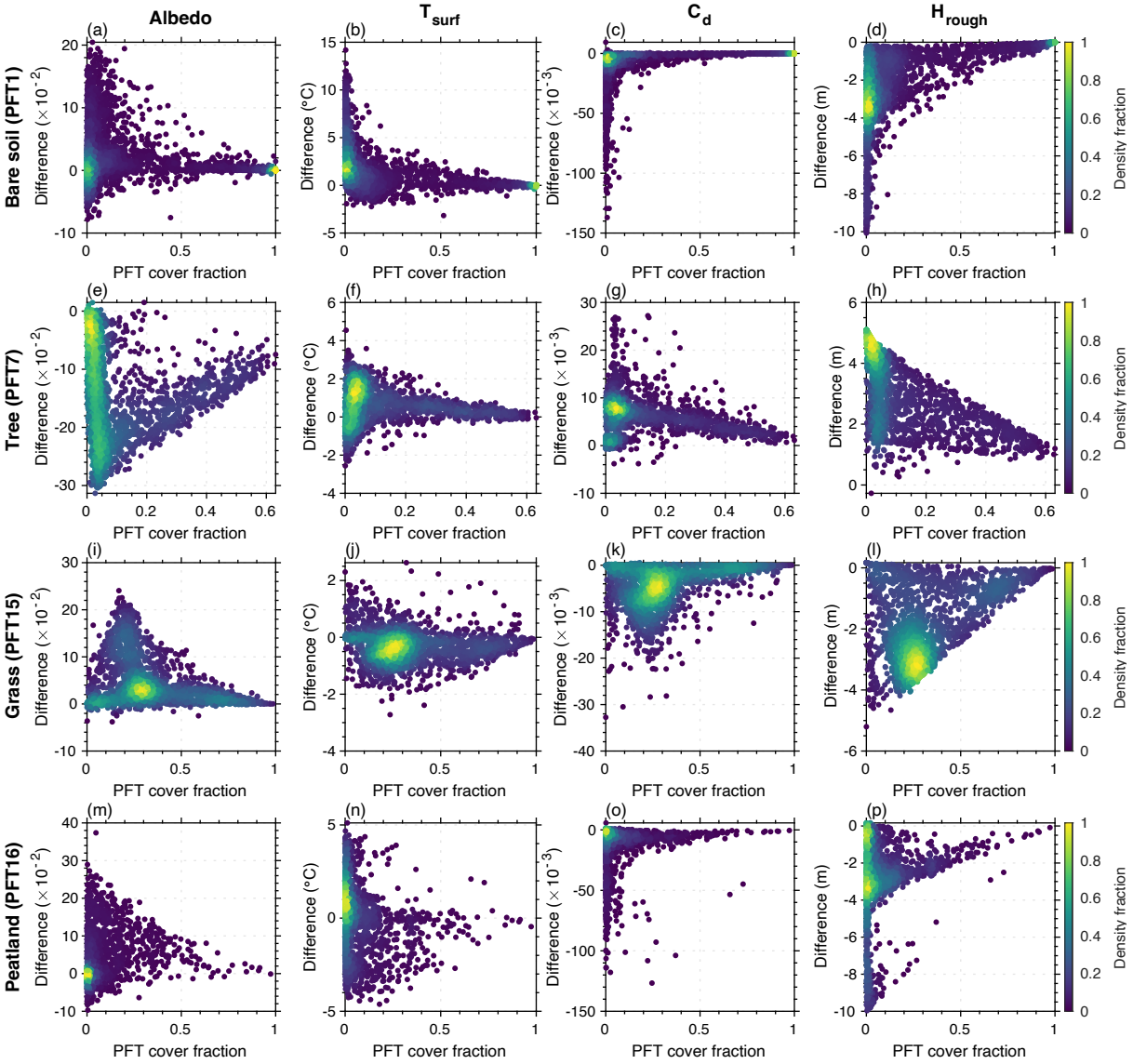

Figure S7. Spatial patterns of relative differences in snow heat capacity (c_{snow}) between MICT-teb and MICT for three snow layers and the snow depth weighted results over the Northern Hemisphere.

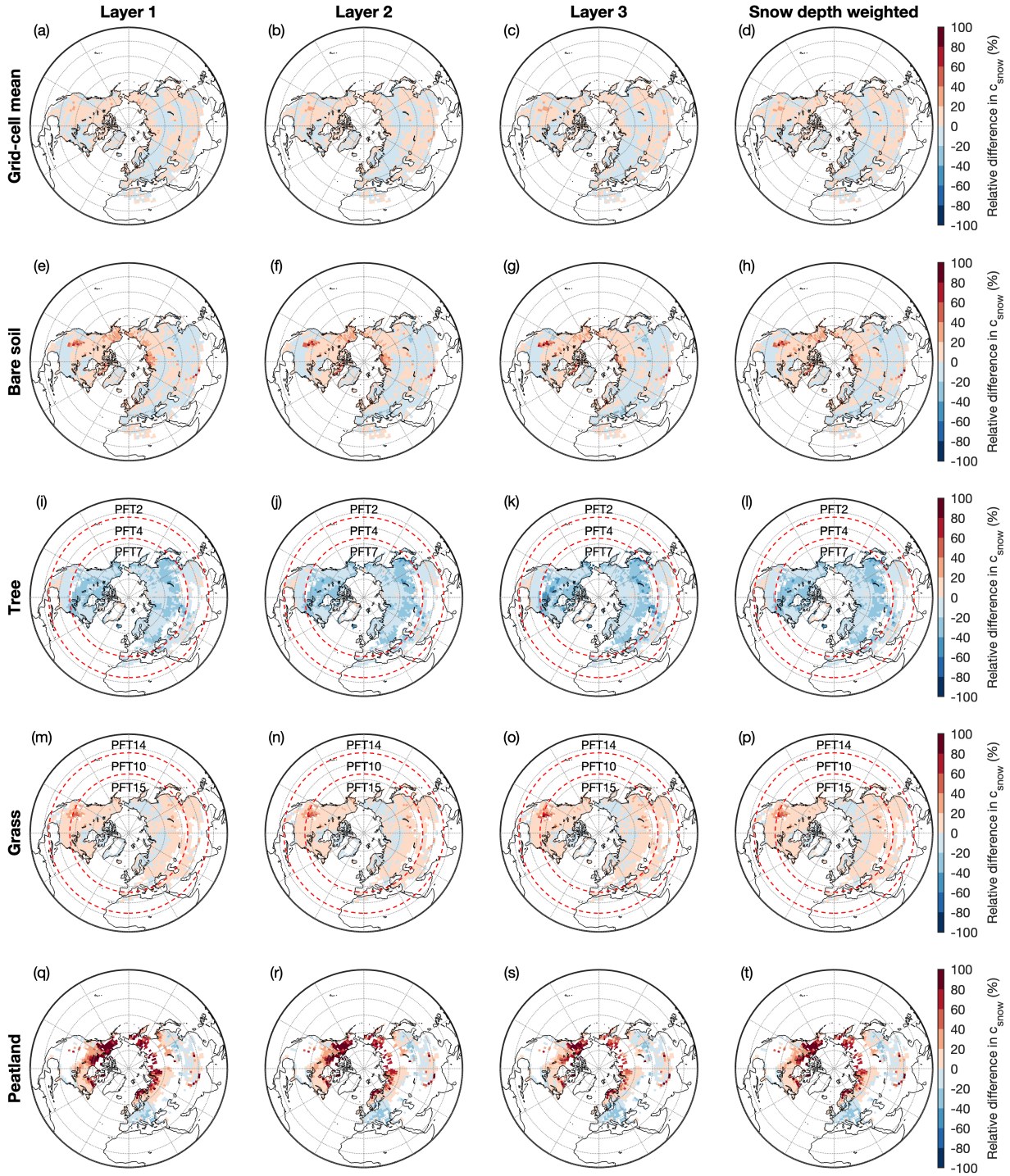

Figure S8. Spatial patterns of relative differences in snow thermal conductivity (λ_{snow}) between MICT-teb and MICT for three snow layers and the snow depth weighted results over the Northern Hemisphere.

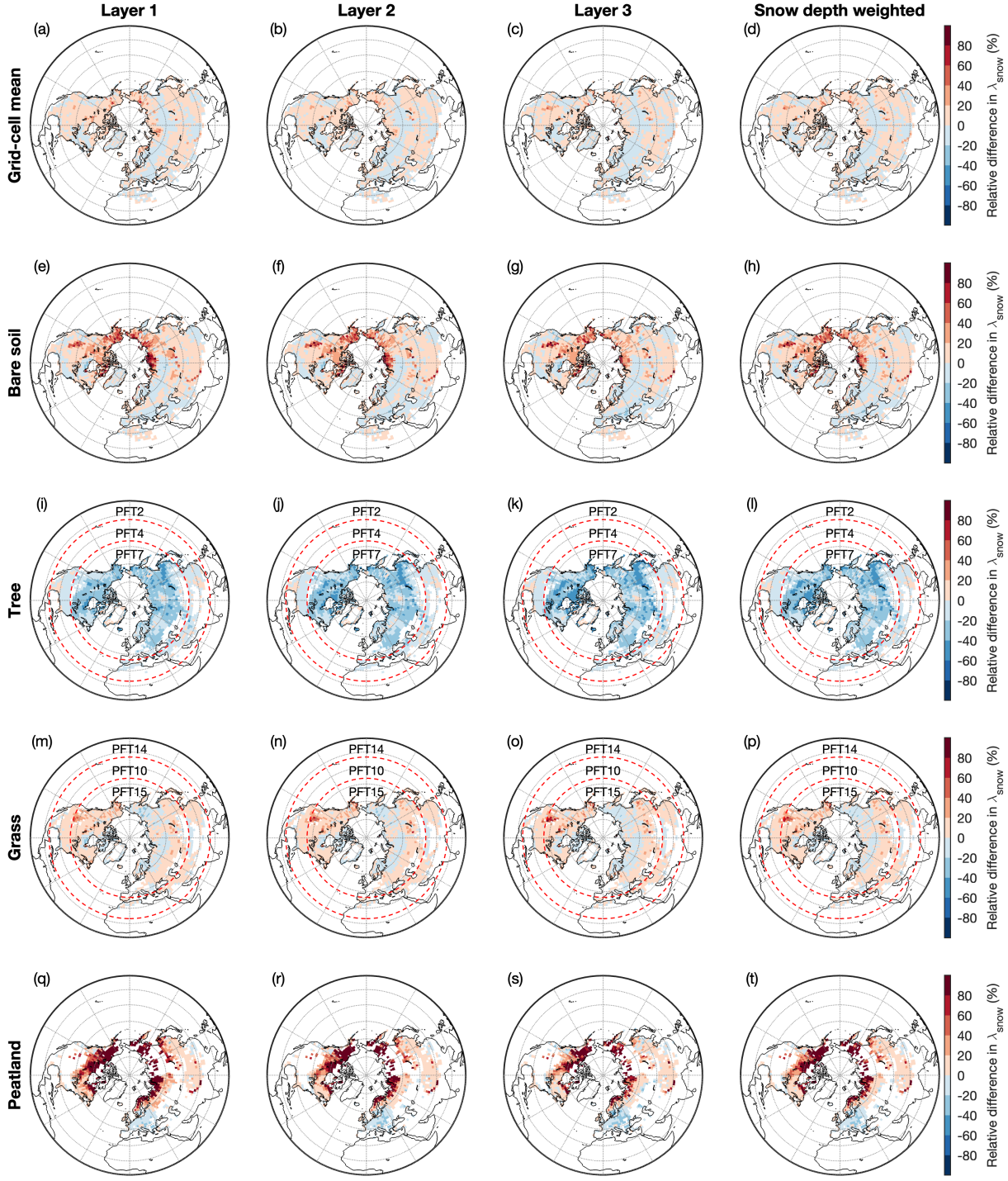

75

Figure S9. Spatial patterns of relative differences in soil heat capacity (c) between MICT-teb and MICT for four soil layers over the Northern Hemisphere.

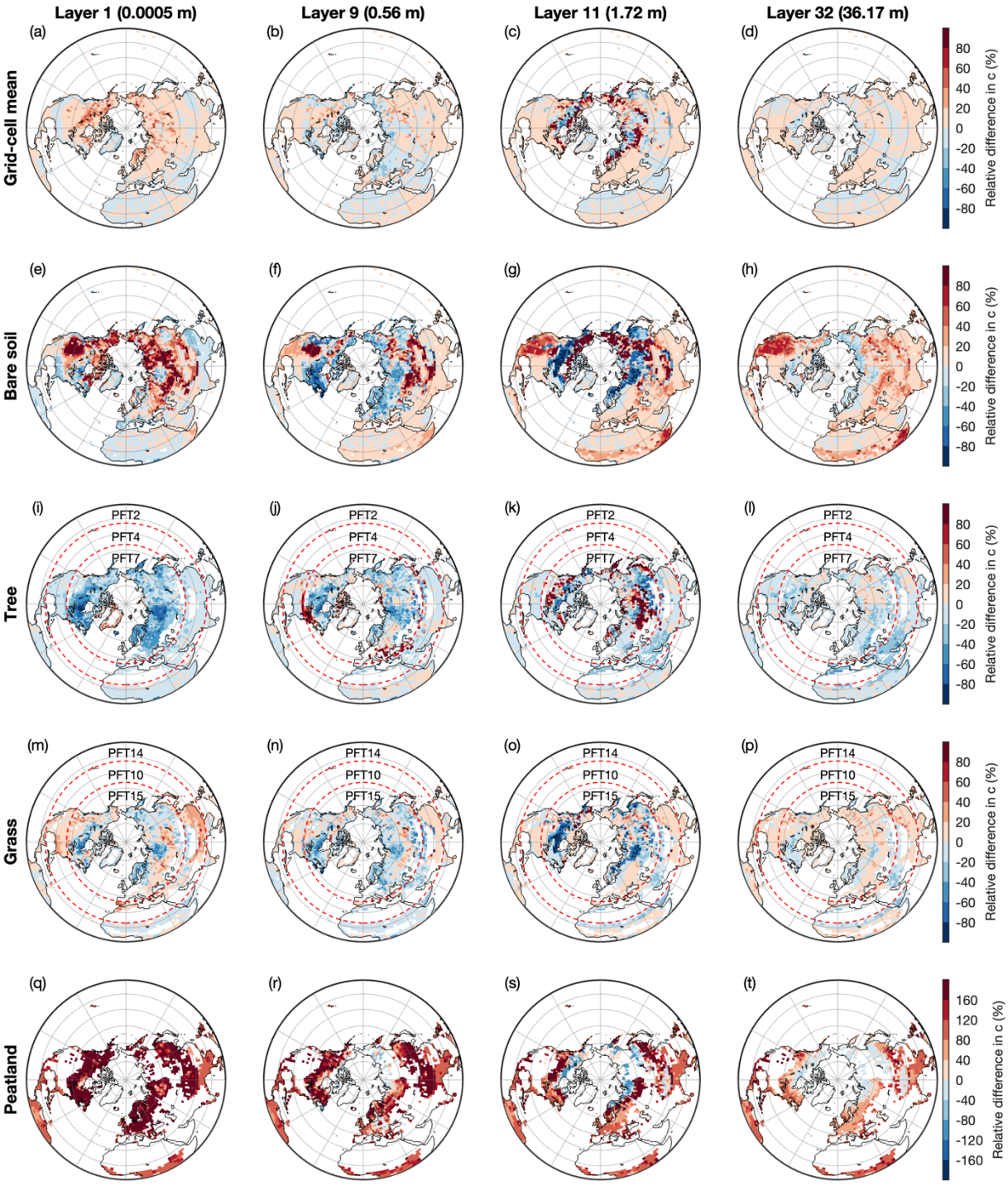

Figure S10. Spatial patterns of relative differences in soil thermal conductivity (λ) between MICT-teb and MICT for four soil layers over the Northern Hemisphere.

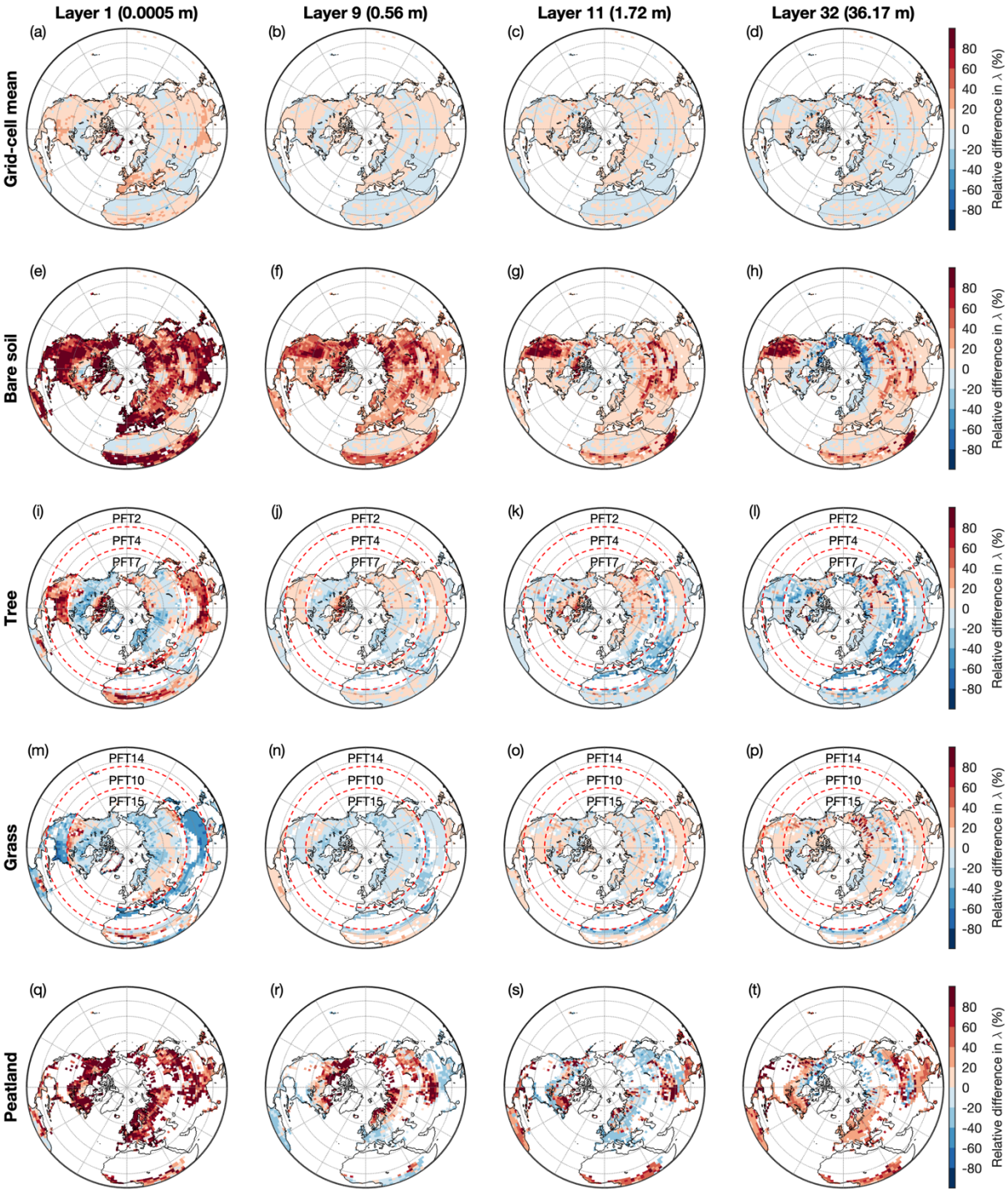

Figure S11. Spatial patterns of relative differences in liquid soil moisture (SM_{liquid}) between MICT-teb and MICT for four soil layers over the Northern Hemisphere. Please note that 1) the hydrology has only 11 layers, so the SM at the 11st layer is used for the 12nd to the 32nd thermal layers to calculate the thermal parameters, and the differences in the third and the last column are resulted from the different soil temperature in the two layers. 2) the MICT distincts SM for different soil tiles, but the grid-cell mean SM is used to calculated soil heat capacity (Fig. S9) and soil thermal conductivity (Fig. S10), so the differences here show the SM_{liquid} for one PFT for MICT-teb and the SM_{liquid} for the total grid-cell for MICT.

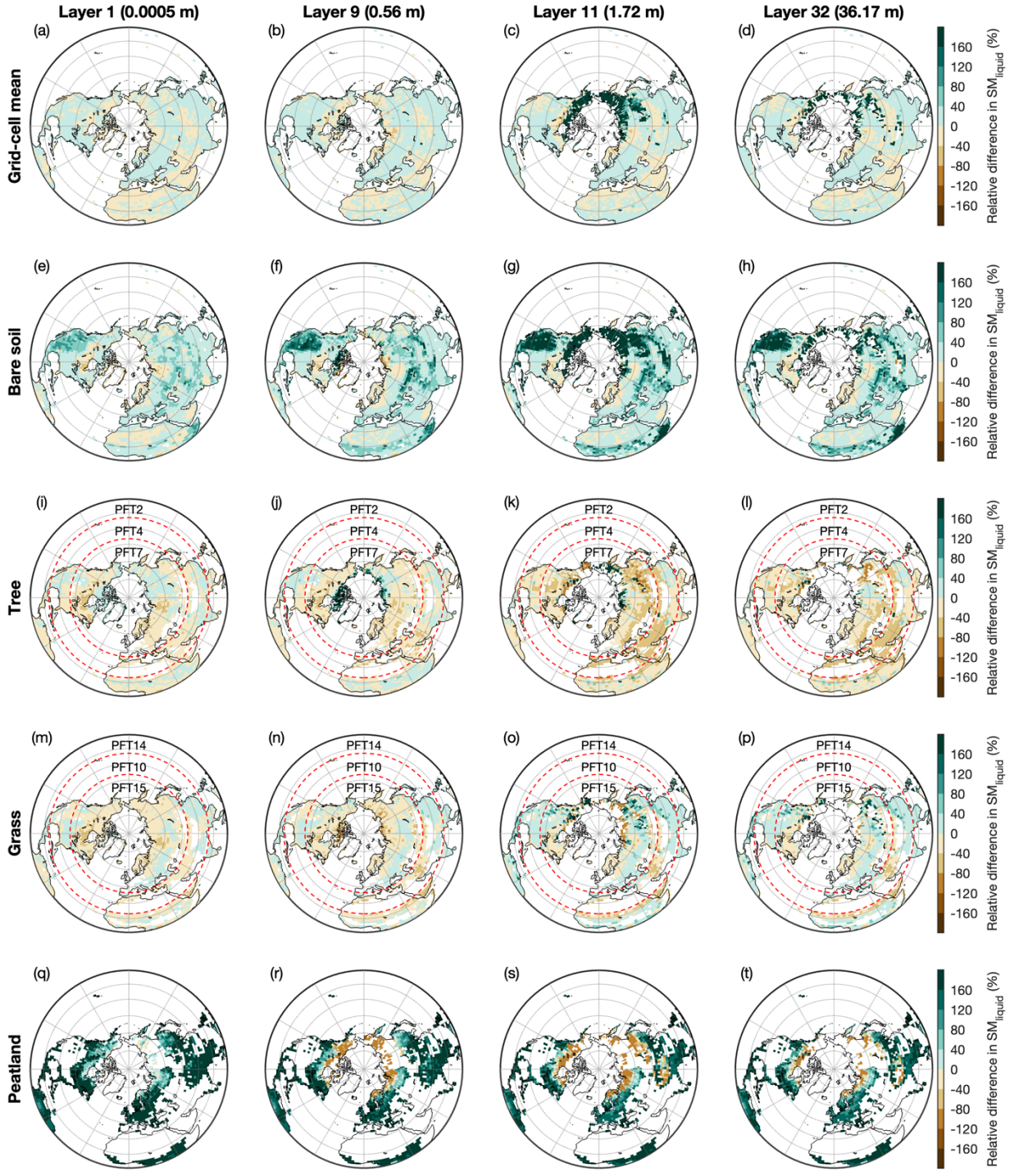
Layer 1 (0.0005 m)
Layer 9 (0.56 m)
Layer 11 (1.72 m)
Layer 32 (36.17 m)
Grid-cell mean
Bare soil
Tree
Grass
Peatland
(a)
(b)
(c)
(d)
(e)
(f)
(g)
(h)
(i)
(j)
(k)
(l)
(m)
(n)
(o)
(p)
(q)
(r)
(s)
(t)
PFT2
PFT4
PFT7
PFT14
PFT10
PFT15
160
120
80
40
0
-40
-80
-120
-160
Relative difference in SM$_{liquid}$ (%)

Figure S12. Same as Fig. S11, but for spatial patterns of relative differences in frozen soil moisture (SM_{frozen}) between MICT-teb and MICT for four soil layers over the Northern Hemisphere.

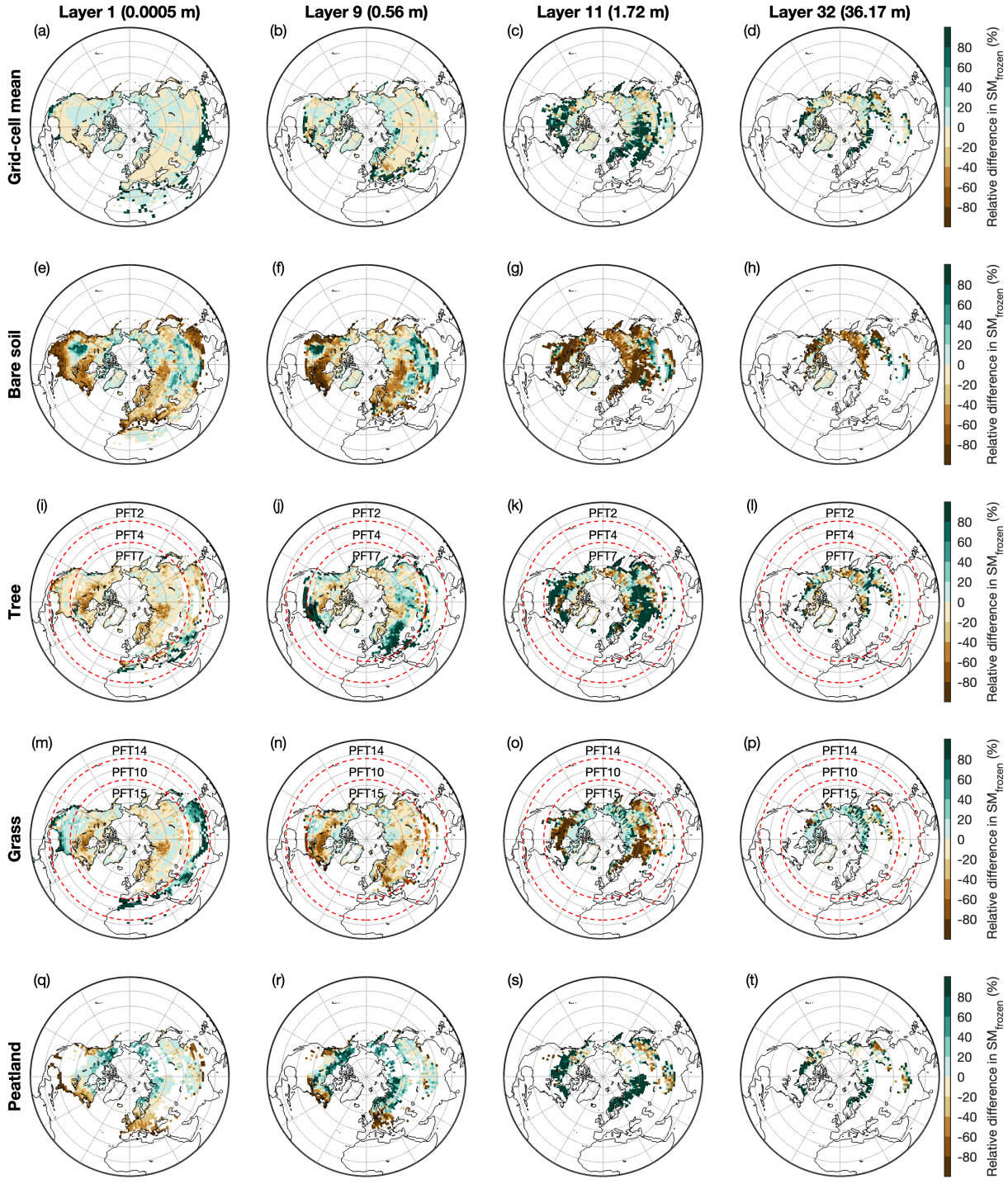

Figure S13. Same as Fig. S11, but for spatial patterns of relative differences in SOC between MICT-teb and MICT for four soil layers over the Northern Hemisphere. The Layer 32 is not shown here because there is no SOC in that layer.

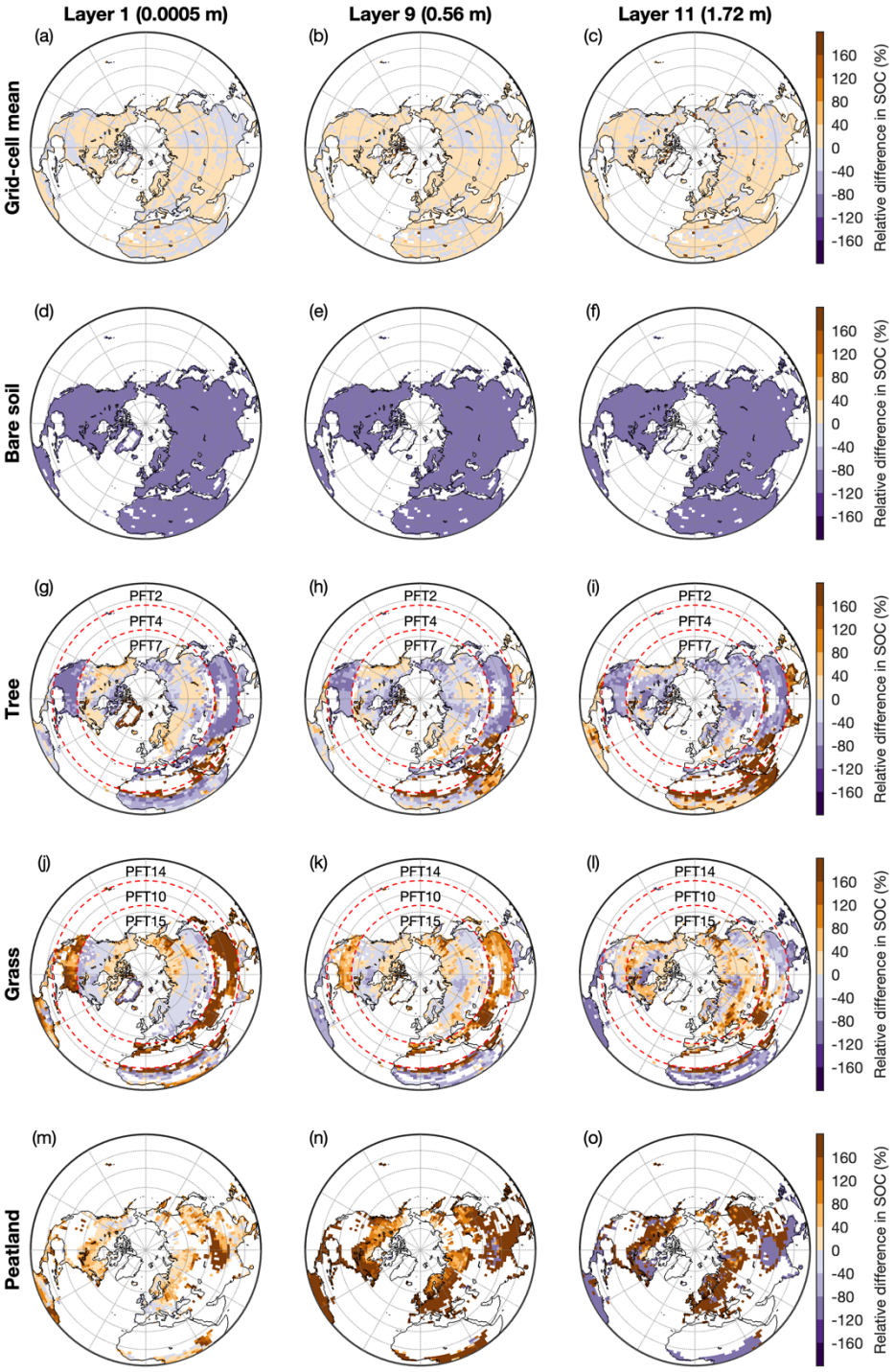

95

Figure S14. Differences in annual evapotranspiration (ET), soil evaporation (E_{soil}), transpiration (E_{trans}), interception (E_{inter}), sublimation (E_{subli}), soil moisture (SM), and snow for four soil tiles between S2 and S0. The annual values are calculated with the average of the last ten years. Considering the different cover fraction of the four soil tiles over the Northern Hemisphere, we use the units of per grid-cell rather than per PFT for the convenience of comparison.

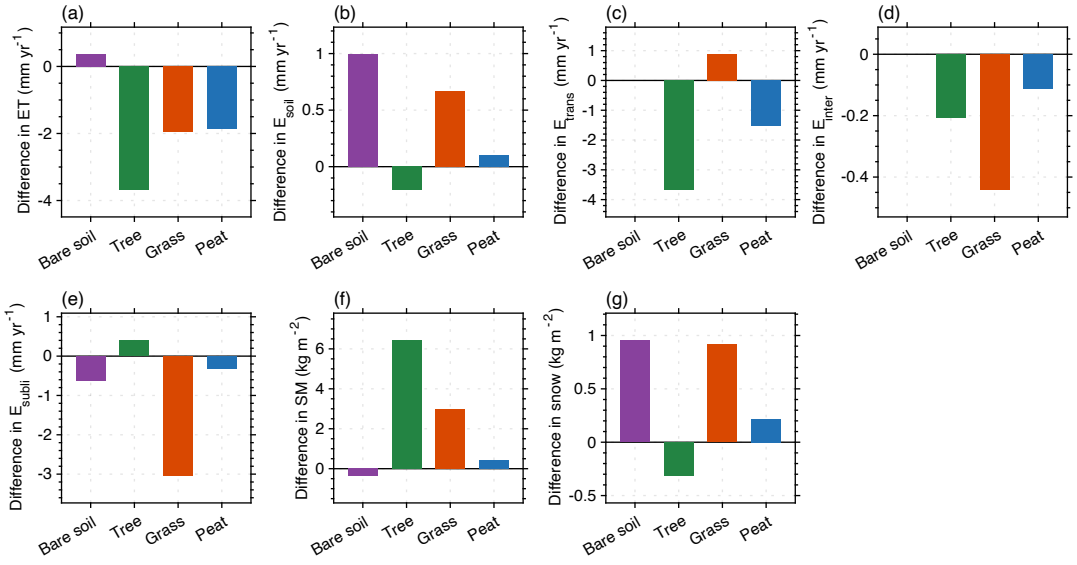

100

Figure S15. Spatial patterns of differences in annual soil evaporation (E_{soil}), transpiration (E_{trans}), interception (E_{inter}), and sublimation (E_{subli}) for grid-cell mean and four soil tiles between S2 and S0. Consistent with Fig. S14, the annual values are calculated with the average of the last ten years and the units are per grid-cell. Areas with a zero flux for both S0 and S2 are masked out, for example in Fig. (f) and (g).

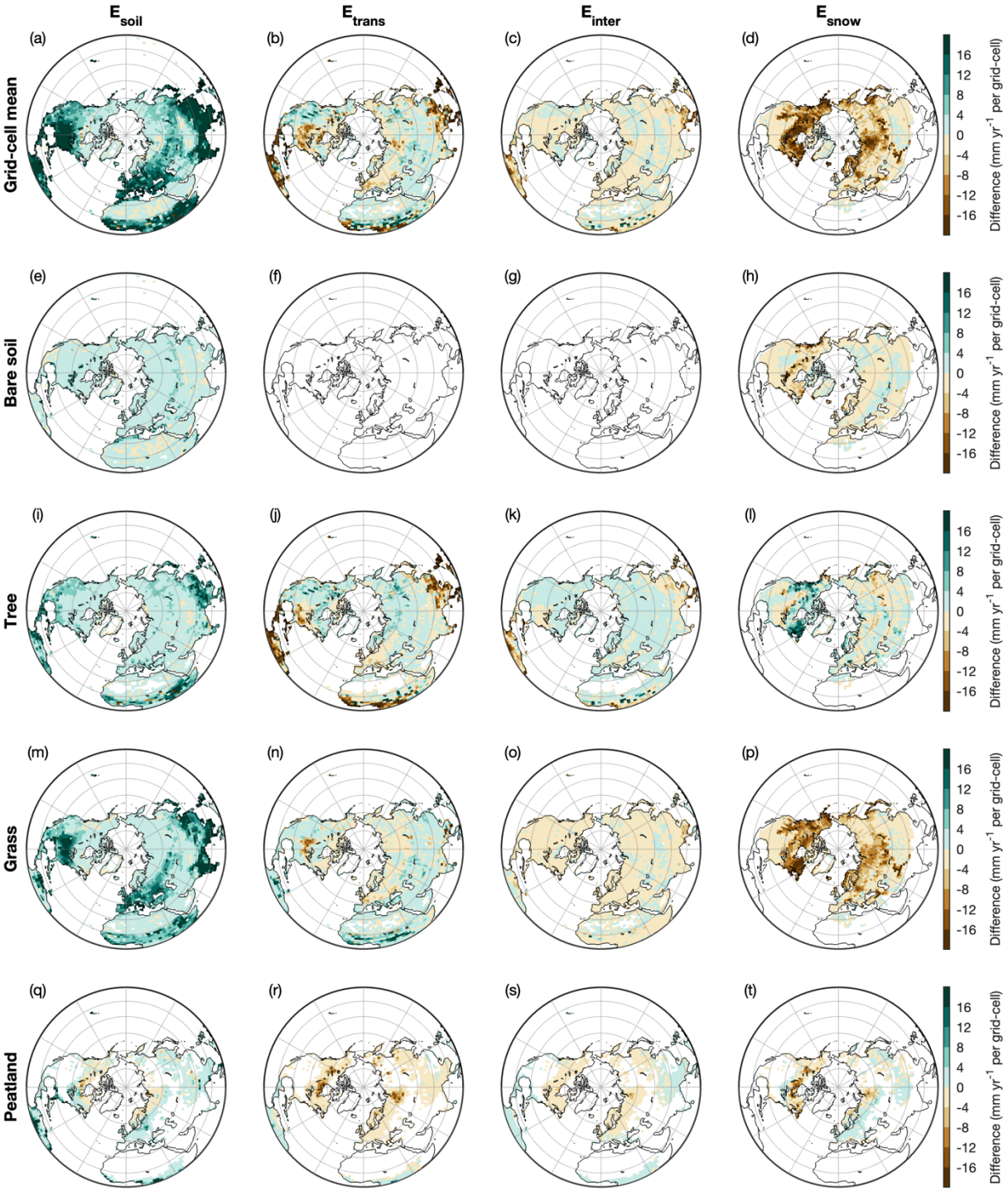
E soil
E trans
E inter
E snow
(a)
(b)
(c)
(d)
Grid-cell mean
(e)
(f)
(g)
(h)
Bare soil
(i)
(j)
(k)
(l)
Tree
(m)
(n)
(o)
(p)
Grass
(q)
(r)
(s)
(t)
Peatland
16
12
8
4
0
-4
-8
-12
-16
Difference (mm yr-1 per grid-cell)

Figure S16. Spatial patterns of differences in annual T_{soil} and SM for grid-cell mean and four soil tiles between S2 and S0. The T_{soil} and SM represent the depth-weighted average for 0-38 m.

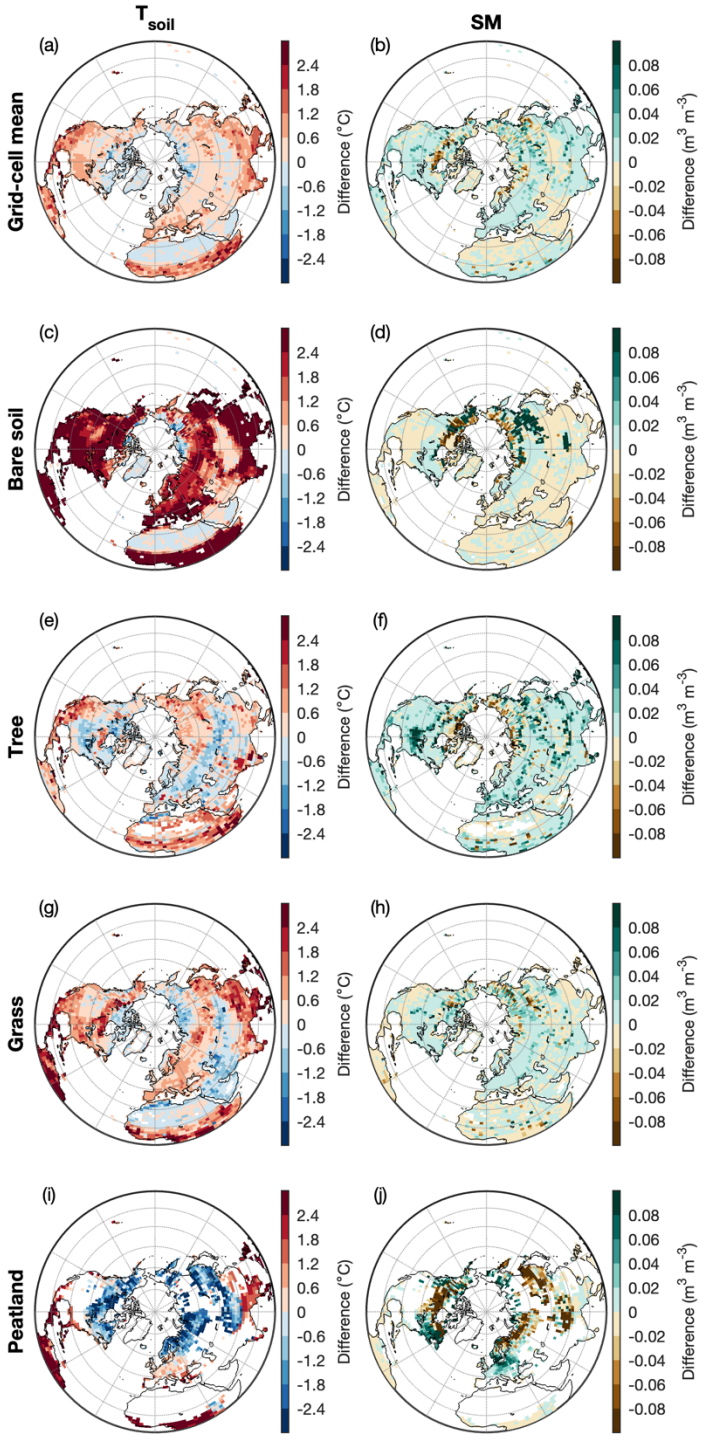

110

Figure S17. Spatial patterns of differences in annual GPP, NPP, R_h, and SOC for grid-cell mean and four soil tiles between S2 and S0. All maps are shown with the units of per grid-cell and the depth for R_h and SOC is 0-38 m.

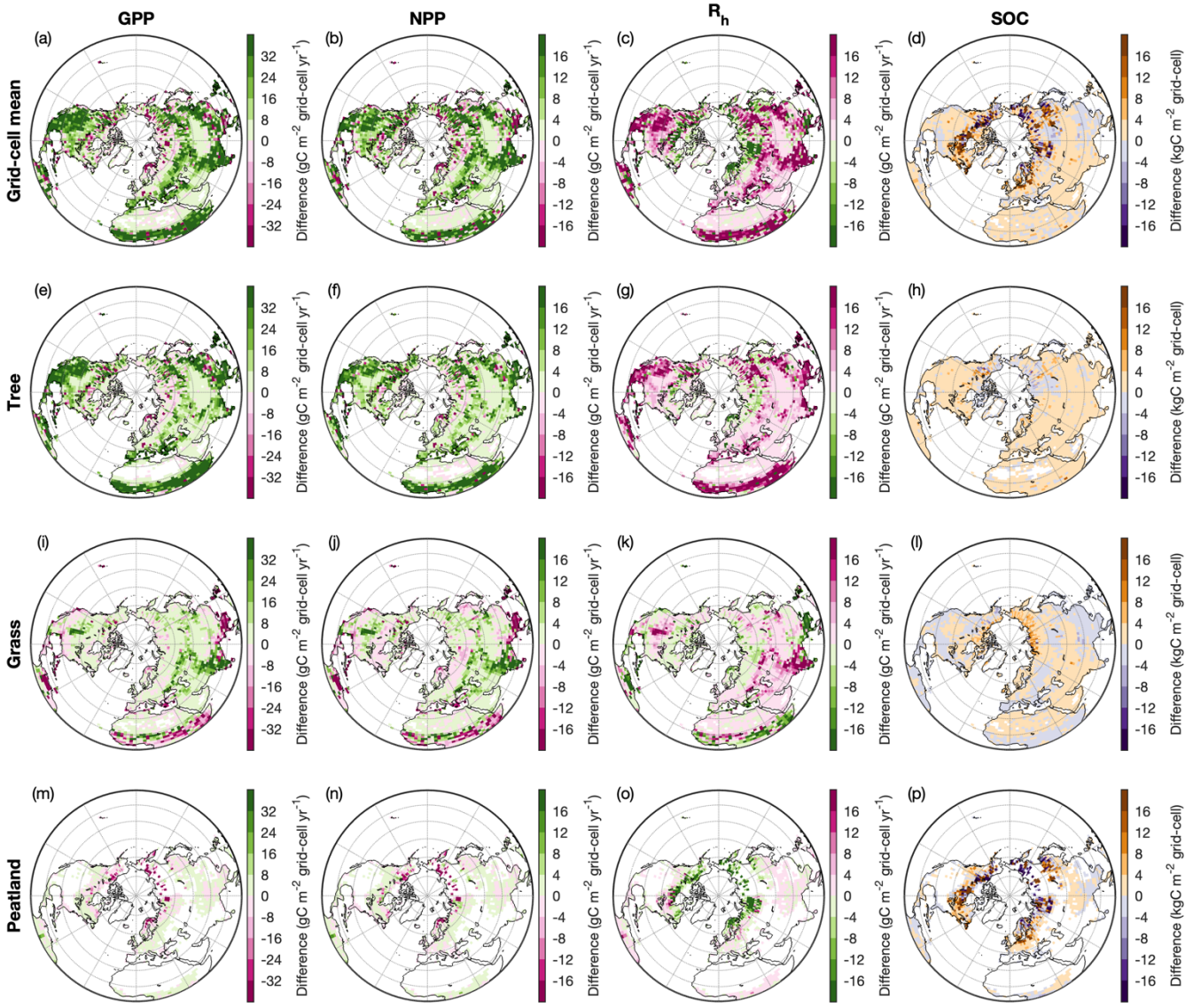

Figure S18. Comparison of land cover maps from simulations in this study and MODIS.

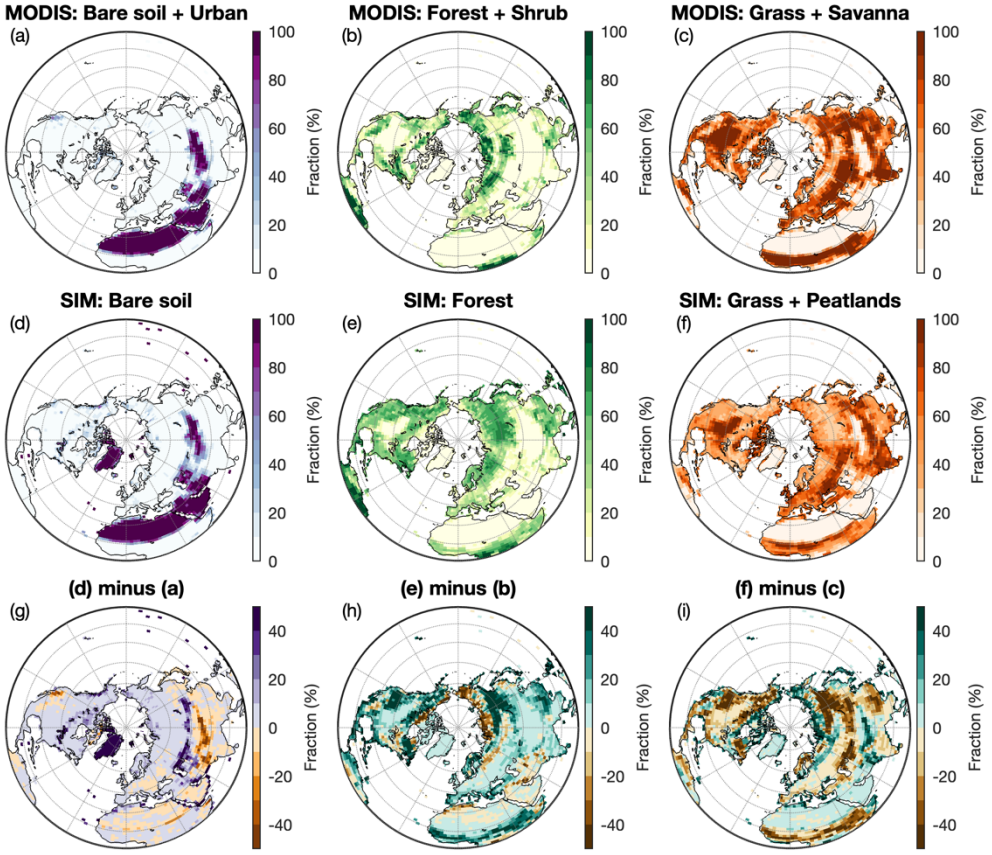

Figure S19. Same as Fig. 15, but for evaluation of simulated soil temperature (T_{soil}) at 20 cm from MICT with site observations.

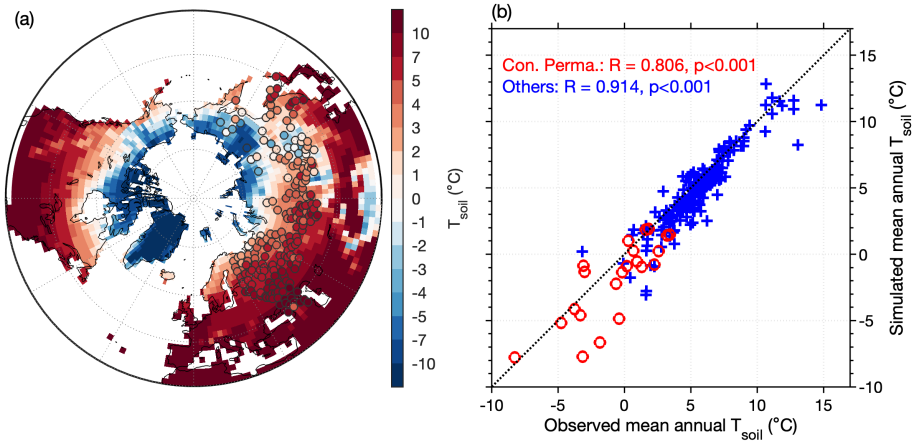

120

Figure S20. Comparison of the bias in soil temperature (T_{soil}) at 20 cm from MICT-teb against site data and the bias in surface temperature (Tsurf) against the MOIDS product. All values in the four figures using the results in the year 2000, the time period covered by the two observation data and simulations.

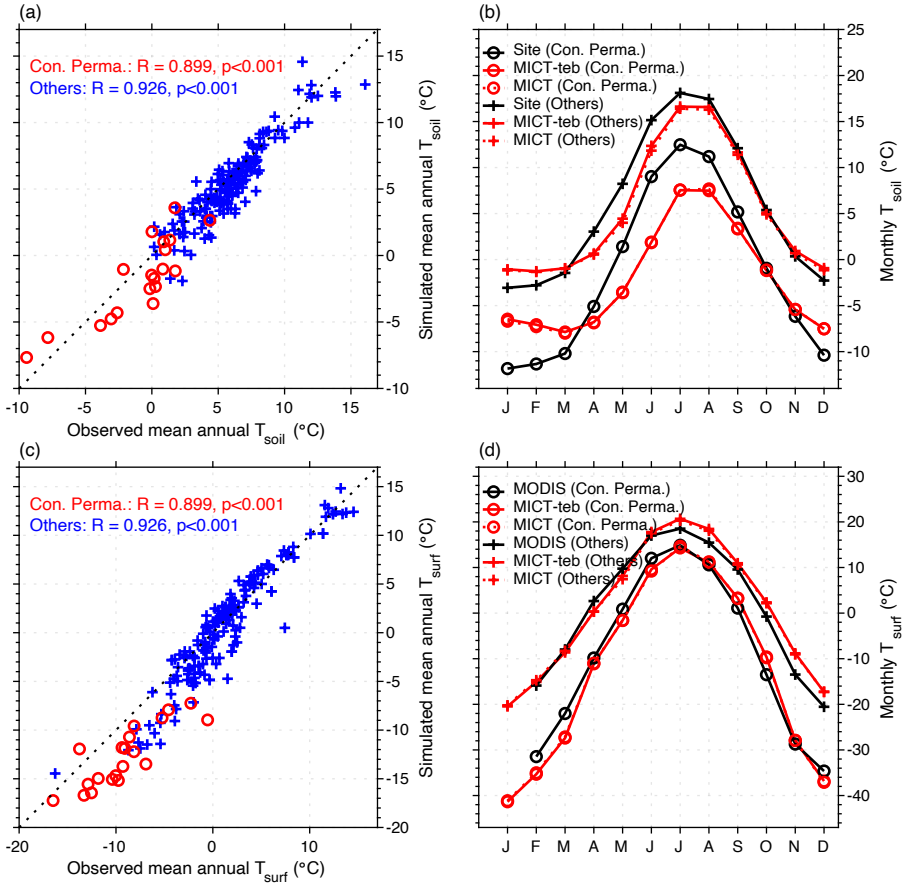

125

Figure S21. Same as Fig. 16, but for the permafrost areas defined by soil temperature.